

1 RESEARCH ARTICLE

2 EARTH SCIENCES

3

4 **Mercury records from natural archives reveal**
5 **ecosystem responses to changing atmospheric**
6 **deposition**

7

8 Qinqin Chen^{1,2}, Qingru Wu^{1,2}, Yuying Cui^{1,2}, Shuxiao Wang^{1,2*}

9

10 ¹ State Key Joint Laboratory of Environmental Simulation and Pollution Control, School of
11 Environment, Tsinghua University, Beijing, 100080, China

12 ² State Environmental Protection Key Laboratory of Sources and Control of Air Pollution
13 Complex, Beijing, 100084, China

14 *Correspondence: shxwang@tsinghua.edu.cn

15 **ABSTRACT**

16 Global ecosystems face mercury contamination, yet long-term data is scarce, hindering
17 understanding of ecosystem responses to atmospheric Hg input changes. To bridge data gap
18 and assess ecosystem responses, we compiled and compared a mercury accumulation
19 database from peat, lake, ice, and marine deposits worldwide with atmospheric mercury
20 deposition modeled by GEOS-Chem, focusing on trends, magnitudes, spatial-temporal
21 distributions, and impact factors. The mercury fluxes in all four deposits showed a five to
22 nine-fold increase over 1700-2012, with lake and peat mercury fluxes generally mirrored
23 atmospheric deposition trends. Significant decreases in lake and peat mercury fluxes post-
24 1950 in Europe evidenced effective environmental policies, whereas rises in East Asia, Africa,
25 and Oceania highlighted coal-use impacts, *inter alia*. Conversely, mercury fluxes in marine
26 and high-altitude ecosystems did not align well with atmospheric deposition, emphasising
27 natural influences over anthropogenic impacts. Our study underscores the importance of these
28 key regions and ecosystems for future mercury management.

29 **Keywords:** Mercury pollution, natural archive, GEOS-Chem, ecosystem recovery, policy
30 evaluation

31 INTRODUCTION

32 Mercury (Hg) is recognized as one of the top ten global pollutants due to its high toxicity and
33 strong tendency to bioaccumulate in the environment [1]. Mercury is mobilized by
34 anthropogenic activities such as metal mining and fossil fuel burning [2, 3], and natural
35 activities such as volcanic eruptions and biomass burning, as well as reemissions from legacy
36 Hg [1]. Emitted Hg primarily exists in a gaseous form (Hg^0) that can travel long distances.
37 During transport, Hg^0 may be oxidised to Hg^{2+} and methylmercury, both of which are more
38 bio-accumulative and water-soluble. These transported Hg are subsequently deposited to
39 terrestrial and marine ecosystems through dry and wet deposition processes, leading to
40 contamination [4]. Once deposited, Hg eventually accumulates in environmental
41 compartments like aquatic sediments and peat [1], posing long-term risks to the ecosystems
42 and human health [5]. To mitigate the adverse effects of Hg, the Minamata Convention on
43 Mercury, an international legally binding treaty, came into force in 2017 [6]. This convention
44 complements national atmospheric protection policies that could synergistically reduce Hg
45 emissions through end-of-pipe controls. Notable examples of these policies include the
46 United Kingdom's Clean Air Act of 1956 and the United States' Clean Air Act of 1970,
47 among the earliest regulations controlling air pollution.

48 Due to these pollution control efforts, recent observations showed reduced Hg emissions and
49 ambient concentrations in the Arctic [7], Europe, and North America [8-10]. However, these
50 reductions in emissions and ambient concentrations might not fully indicate changes in
51 contamination levels within underlying surface ecosystems. Ecosystems include various
52 elements like organisms, waterbodies, and natural deposits, each governed by unique Hg
53 deposition mechanisms. Of particular concern and research interest are natural deposits,
54 including peat, lake sediments, marine sediments, and ice, as they serve as final Hg sinks and
55 potential Hg sources of the respective ecosystems. These natural deposits inherently preserve
56 and accumulate environmental contaminants like Hg in chronological order [11-13] and thus
57 are known as natural archives. In particular, the Hg accumulated in nature archives in
58 undisturbed regions was considered to be primarily sourced from atmospheric depositions
59 [14]. Therefore, such long-term natural archive Hg records are valuable for studying how
60 respective ecosystems, particularly their natural deposit component, respond to changing
61 atmospheric Hg deposition.

62 Different types of natural archives may not respond the same to the changing atmospheric
63 inputs due to unique Hg deposition processes. For instance, Hg in peat is primarily from
64 atmospheric deposition, which encompasses vegetation uptake through active absorption by
65 plant roots and foliage [15-19] and is influenced by peat growth and microbial decomposition

66 [20]. In lake sediments, Hg accumulates from direct atmospheric deposition including
67 vegetation fixation and catchment runoff, including legacy Hg from catchment soil [21-23].
68 Marine sediments acquire Hg through a balance of atmospheric deposition and reemissions,
69 with waterbodies [24] and sea ice as natural barriers to Hg exchange [25]. Coastal erosion can
70 also contribute to Hg inputs in marine sediments [26]. In ice sheets and glaciers, Hg
71 accumulates primarily through atmospheric deposition. Significant photoreduction of Hg [27],
72 along with ice sublimation and melting [27-29], contributes to annual Hg deposition loss. SI
73 Table S1 summarised major depositional processes of Hg to peat, lake sediments, marine
74 sediments and ice. Previous studies reviewed Hg records from natural archives like peat and
75 lake sediments and offered qualitative assessments at regional and hemispheric scales [30-33]
76 (see SI Supporting Text 1). However, these studies were limited in providing quantitative
77 comparisons across ecosystems and regions. Such comparisons would be invaluable for
78 understanding different ecosystem responses, evaluating the effectiveness of source-control
79 policies, and informing future mitigation strategies.

80 In this study, we aim to utilize the Hg records from natural archives along with atmospheric
81 modelling to understand how different ecosystems, at least their natural deposit components
82 acting as the Hg sinks, respond to changing atmospheric Hg deposition. First, we compiled a
83 natural archive Hg database from 1700 to 2012. The database consisted of Hg accumulation
84 fluxes of 221 cores extracted from ice, peat, lake, and marine deposits. These deposits,
85 primarily influenced by atmospheric Hg deposition, were sampled from eight key regions
86 worldwide, covering the period from 1700 to 2012. Second, we compared the trends, rates,
87 and magnitudes of Hg accumulation in four natural archives throughout 1980-2012 to the
88 respective atmospheric Hg deposition modelled by GEOS-Chem. This comparison elucidated
89 how Hg levels in these archives respond to atmospheric changes, thereby enhancing our
90 understanding of Hg records across eight key regions. Last, based on the unique responses of
91 natural archives across regions, we discussed policy effectiveness and highlighted key regions
92 and ecosystems that may require more targeted Hg management strategies.

93 **RESULTS AND DISCUSSION**

94 **Natural Archive Mercury Database**

95 We meticulously selected 221 cores primarily impacted by atmospheric Hg deposition, as
96 indicated in the respective literature (Fig. 1a, see detailed Method in Supporting Text 2, SI
97 Fig. S1-3, and Dataset S1). The core selection was based on five stringent criteria, including
98 the requirements that the cores be free from significant physical and chemical disturbances,
99 provided Hg accumulation flux ($\text{mg}/\text{m}^2/\text{yr}$), and covered the period from 1700 to 2012 with a

100 temporal resolution finer than 20 years, considering potential chronological errors. These
101 selected cores were categorized into eight key regions, with the highest number of cores from
102 North America (47%), followed by Europe (11%), the Arctic (11%, mainly Greenland), Latin
103 America (9%, mainly Central America and the western Andes), Central Asia (8%, mainly
104 Tibetan Plateau), East Asia (6%), Central and Southern Africa (3%), and Oceania (2%) (see
105 SI Table S2 for a full list). In terms of core types, 72% were lake cores (distributed globally),
106 followed by peat cores (13%, mainly in Europe), marine cores (11%, in continental shelf
107 areas), and ice cores (4%, in polar and mountainous regions).

108 Cores from different studies exhibit varying temporal scales, which can significantly impact
109 the accuracy of regionally synthesized data. This inconsistency affects the precision of
110 annually averaged Hg accumulation flux data within each region. To resolve this issue, we
111 employed the General Additive Model (GAM), which offers flexibility by allowing for non-
112 linear relationships between predictors and the response variable [34]. This approach enabled
113 the prediction of Hg accumulation fluxes up to 2012 for cores whose uppermost layers did not
114 date to the year 2012, thereby ensuring temporal consistency and enhancing the accuracy and
115 reliability of our Hg flux predictions. We fed GAM with selected eight predictors (detailed in
116 Table S4): local anthropogenic emission, local non-anthropogenic emission (i.e., natural
117 emissions and re-emissions), global total emission, surface temperature, precipitation,
118 greenness fraction, elevation (or depth for marine cores), and the ratio between catchment
119 area and lake area (applicable only for lake cores). The GAM analysis established correlations
120 between these predictors and Hg accumulation fluxes in each of the four types of natural
121 archives. The GAM result showed that the four correlations explained 65%, 88%, 85%, and
122 83% of the deviances in lake, peat, marine and ice deposits, respectively (Table 1, SI Fig. S4-
123 12). Based on the established four correlations, we predicted the Hg accumulation flux data
124 for each core that does not extend to 2012.

125 Combining the Hg accumulation flux data extracted from literature and the GAM predictions,
126 we compiled a natural archive Hg database from 1700 to 2012 (referred to as “the database”).
127 The database showed distinctive patterns of Hg accumulation fluxes in the four types of
128 natural archives over the last three centuries. The averaged Hg fluxes in peat, lake, ice, and
129 marine cores, hereafter referred to as “peat-Hg fluxes”, “lake-Hg fluxes”, “ice-Hg fluxes”,
130 and “marine-Hg fluxes”, have increased by five-fold, six-fold, eight-fold, and nine-fold,
131 respectively, culminating in peak contemporary levels at 0.033 ± 0.034 mg/m²/year, $0.055 \pm$
132 0.123 mg/m²/year, 0.002 ± 0.004 mg/m²/year, and 0.124 ± 0.175 mg/m²/year (mean \pm
133 standard deviation, detailed data in SI Table S3). These substantial variations in changing
134 rates and magnitudes highlight the differences among Hg deposition mechanisms in the four
135 types of natural deposits and reflect the key responses of those Hg sinks of each ecosystem to

136 the changing atmospheric Hg deposition. Therefore, the following sections further discuss
137 these responses by analysing the deviances and similarities between each type of natural
138 archive Hg accumulation and respective atmospheric Hg deposition. These responses help to
139 further understand the changes in Hg accumulation in key regions.

140 **Responses of lake and peat core records to changing atmospheric deposition**

141 *Lake-Hg and peat-Hg fluxes generally changed with atmospheric Hg deposition*

142 We compared the natural archive Hg accumulation fluxes to the GEOS-Chem modelled
143 atmospheric Hg deposition at each of the coring locations (Fig. 1b and SI Fig. S13). The
144 GEOS-Chem model was driven by EDGAR anthropogenic Hg emissions [35] and MERRA2
145 meteorological data [36]. The modelling generated atmospheric Hg deposition fluxes (total,
146 wet, and dry) in $2^{\circ} \times 2.5^{\circ}$ grids, which offer a cost-effective balance between simulation
147 accuracy and computational efficiency. Model validation against observations indicated an
148 acceptable error margin of approximately 50% (SI Fig. S13). Our comparison revealed that
149 lake and peat cores exhibited similar figures, with 45% of lake-Hg fluxes and 46% of peat-Hg
150 fluxes between 1980 and 2012 falling within a one-fold range of their respective modelled
151 total atmospheric deposition fluxes (SI Fig. S14). However, extremes were noted: 7% of lake-
152 Hg fluxes (11 cores) and 7% of peat-Hg fluxes (2 cores) deviated by more than ten-fold,
153 surpassing the modelled deposition. Additionally, 55% of lake cores and 48% of peat cores
154 exhibited Hg accumulation trends that aligned with their respective modelled deposition
155 trends over the same period.

156 Apart from the similarities mentioned above, the key impact factors influencing both lake-Hg
157 and peat-Hg fluxes also showed similar patterns, despite their distinctive deposition
158 mechanisms. We analysed the impact of eight relevant environmental, geographical, and
159 emission-related factors on the changes in lake-Hg and peat-Hg fluxes using the GAM
160 approach (See SI Supporting Text 2 for methods). The analysis revealed that local
161 anthropogenic Hg emissions had the most significant impact on both lake-Hg and peat-Hg
162 fluxes, evidenced by the highest F values among all factors, with temperature being the next
163 most influential factor (Table 1). The fact that lake-Hg and peat-Hg fluxes share the same
164 primary and secondary impact factors is likely because lakes and peatlands are both covered
165 by generally stagnant water and these cores were taken from relatively remote areas with
166 limited external disturbances. These conditions make atmospheric deposition the dominant
167 input to these natural archives, making them more susceptible to local atmospheric emissions.
168 The significance of temperature is due to its impact on disrupting biogeochemical cycles of
169 Hg within lake and peat ecosystems. For instance, rising temperatures can promote vegetation
170 growth and aquatic system productivity. These changes could lead to an increase in

171 vegetation fixation and the input of organic matter-bound Hg to peat and lake sediments [18,
172 37]. Besides, rising temperatures could contribute to glacier retreat, providing additional Hg
173 input from meltwater to proglacial lakes [29, 38, 39].

174 The general concordance in trends and magnitudes between the modelled data and lake-Hg
175 and peat-Hg fluxes suggests that both types of natural archives are responsive to changes in
176 atmospheric Hg depositions. Besides, the shared key impact factors, particularly local
177 anthropogenic emissions, indicate that lake and peat cores could be used in tandem to assess
178 the impact of anthropogenic activities, such as the onset of major industries and the
179 implementation of pollution control policies. In the following subsection, we leverage this
180 knowledge to discuss regional changes in lake and peat records.

181 *Regional lake and peat records reflected contemporary anthropogenic impact*

182 From 1900 onwards, lake-Hg and peat-Hg fluxes in all regions started to rise, but their
183 trajectories diverged after the 1950s. Europe was the only region showed significant reduction,
184 with lake-Hg and peat-Hg fluxes decreasing by 94% and 97%, respectively, from the
185 respective peaks in the 1950s and 1970s to 2012 (**Fig. 2a**). In 2012, fluxes dropped to 0.039
186 [0.026, 0.052] (mean [CI2.5%, CI97.5%]) mg/m²/year in lake cores and 0.022 [0.014, 0.030]
187 mg/m²/year in peat cores. These 2012 levels closely resemble preindustrial levels, where the
188 lake-Hg flux was 0.027 [0.015, 0.039] mg/m²/year in 1866 and the peat-Hg flux was 0.006
189 [0.004, 0.008] mg/m²/year in 1760 (the earliest year with multiple cores). The significant
190 reductions observed in lake and peat cores in recent decades align well with the decreasing
191 trends and rates of modelled total atmospheric Hg depositions during 1980-2012 (Table 2 and
192 SI Fig. S15) and with observed Hg⁰ concentration and Hg²⁺ wet deposition during 1990-2010
193 [10]. Besides, the reduction rate of lake-Hg (-1.7%/yr) closely mirrored the modelled
194 reduction rates (-1.6%/yr). These general concurrences in decreasing trends and rates between
195 lake and peat cores indicate that similar factors drove these changes. One major driver
196 contributing to these reductions could be the effective implementation of environmental
197 policies aimed at reducing air pollutant emissions from coal burning in Europe. These policies
198 trace back to the United Kingdom's Clean Air Act of 1956, which was prompted by the Great
199 London Smog and has been strengthened by a series of regulations enacted by the European
200 Union since 1970 [40]. Consequently, most European countries have progressively decoupled
201 their economic development from coal consumption (SI Fig. S16).

202 North America exhibits a mixed flux trend, with lake-Hg fluxes initially increasing at a rate of
203 1.8% per year until the 1970s, followed by a statistically insignificant decrease (**Fig. 2b**). By
204 2012, the lake-Hg flux reached 0.023 [0.021, 0.025] mg/m²/year, representing a five-fold
205 enrichment from the preindustrial level of 0.005 [0.0042, 0.0061] mg/m²/year in the year

206 1700. These overall insignificant decreasing trends in North America result from diverse
207 changing patterns of lake-Hg and peat-Hg trends across its subregions. **Fig. 3** illustrates the
208 spatial-temporal changes in Hg accumulation in North America, derived from GAM analysis
209 (See SI Supporting Text 2 for methods). The result showed declining Hg accumulation fluxes
210 on the eastern and western sides of North America and increasing Hg accumulation fluxes
211 with slowing year-on-year changing rates in the central region during 1980-2012. These non-
212 uniformed subregional trends from natural archives align with the general decreasing patterns
213 in wet deposition observed in the eastern and western regions of the United States, alongside
214 the increasing [41] or slowing decreasing trends [10] in the central region depending on
215 targeted periods. The mixed trends are likely a result of locally specific environmental
216 regulations, including the United States' Clean Air Act of 1970, the continuous reliance on
217 coal in the United States until 2008 (SI Fig. S16), and contributions from transboundary Hg
218 pollution across continents [41].

219 Unlike the declines observed in Europe and North America, lake-Hg fluxes in Oceania,
220 central and southern Africa, and East Asia have experienced intensified Hg accumulation up
221 until 2012 (**Fig. 2c-e**). The recent increases in lake-Hg fluxes agree with the modelled
222 atmospheric deposition during 1980-2012. The increases were likely driven by escalated coal
223 usage in Australia, South Africa, and China, which rose by 71%, 190%, and 533%,
224 respectively, over the same period [42]. Additional contributions to these increases could
225 stem from Artisanal and Small-Scale Gold Mining (ASGM) activities, which are currently the
226 largest Hg emission source [1]. Triggered in part by surging gold prices after the 2000s,
227 ASGM has proliferated in developing regions worldwide, including central and southern
228 Africa and China [43, 44]. However, the magnitude of ASGM emissions carries substantial
229 uncertainties and needs further validation (see SI Supporting Text 4 for more discussion).

230 In Central Asia, high-altitude lake-Hg fluxes remained constant from the 18th century to the
231 1930s and then increased steadily to 2012, standing at 0.020 [0.013, 0.027] mg/m²/year (**Fig.**
232 **2f**). Central Asia is an extensive mountainous region spanning the Third Pole area. Therefore,
233 the region is influenced by global mercury emissions, particularly from neighbouring regions
234 of East Asia and South Asia, both of which have experienced increasing anthropogenic
235 emissions [45]. The high-altitude lake-Hg flux trend aligned with the rising emission trends,
236 as expected. However, the lake-Hg fluxes had a year-on-year changing rate of 1.3%/year
237 during 1980-2012, which surpassed the modelled atmospheric deposition rate of 0.7% at lake
238 locations. This acceleration in high-altitude lake-Hg changing rate could be attributed to a
239 heightened atmospheric supply of oxidated Hg²⁺ at higher elevations due to the increased
240 availability of oxidants [46-49]. Additionally, high-altitude proglacial lakes also receive Hg

241 inputs from glacier meltwater, which have been enhanced by rising temperatures over recent
242 decades [29, 39].

243 **Responses of marine core records to changing atmospheric deposition**

244 *Marine cores generally overstated atmospheric Hg deposition*

245 In contrast to fluxes in lake and peat cores, marine-Hg fluxes significantly differed from the
246 modelled atmospheric deposition in trends and displayed significant differences in
247 magnitudes. Notably, 58% of marine-Hg fluxes between 1980 and 2012 showed disparities
248 exceeding ten-fold, with only 19% of marine-Hg fluxes falling within the one-fold range of
249 the respective total atmospheric Hg deposition fluxes. In general, marine-Hg fluxes were
250 around 20-fold greater than the modelled deposition (SI Fig. S14). These substantial
251 differences between marine-Hg fluxes and modelled atmospheric deposition suggest that the
252 factors driving the changes in atmospheric deposition, such as emission control policies, are
253 not the primary drivers of marine-Hg fluxes. This observation is further supported by the
254 GAM impact factor analysis, which revealed that the ocean depth at the sampling location
255 exerted the most significant impact. Ocean depth can alter the marine-Hg fluxes by
256 influencing the physical movement of marine sediments, to which Hg binds. These
257 movements include sediment focusing [50] and sediment export to the deep sea [51, 52].
258 Eventually, the discrepancies in trends and magnitudes between the modelled data and
259 sedimentation records suggest that marine-Hg fluxes are unlikely to respond in a timely or
260 consistent manner to changes in atmospheric deposition.

261 *All regional marine cores showed rising trends*

262 Marine-Hg fluxes in the oceans of Europe, the Arctic, and East Asia all exhibited increasing
263 trends. These rises are especially noteworthy for Europe and the Arctic, where atmospheric
264 deposition trends were decreasing. In Europe, marine cores showed a significant upward trend
265 of 3% per year before the 1960s, which then slowed to 0.4% per year until 2012. This
266 increasing trend starkly contrasts with the previously discussed declines in the region's
267 modelled atmospheric deposition and the lake-Hg and peat-Hg fluxes following the pivotal
268 periods of the 1950s and 1970s, respectively. By 2012, marine-Hg fluxes in Europe reached
269 0.144 [0.140, 0.148] mg/m² per year, ranking among the highest levels within the database.

270 Similarly, the marine-Hg fluxes in the Arctic showed significant monotonical increasing
271 trends from 1920 to 2012, although the growth rate decreased from 2.8%/year to 0.6%/year
272 after 1980 (**Fig. 2g**). This contemporary increasing trend contrasted with the region's
273 decreasing ambient atmospheric Hg concentration, which has declined by -0.95%/year since

274 1995 based on data from Station Alert at the northern tip of Greenland [7]. The increasing
275 trend also opposed the decreasing modelled atmospheric deposition rate of -0.2%/year during
276 1980-2012, averaged from marine core locations. By 2012, marine-Hg fluxes in the Arctic
277 stood at 0.108 [0.077, 0.140] mg/m²/year, designating it as a Hg accumulation hotspot as
278 shown in Fig. 3.

279 The sustained rises in marine-Hg fluxes in both the Arctic and Europe could be attributed to
280 various factors. These include the continuous cycling of Hg within the marine environment
281 [53], continuous inputs from coastal erosions [26], and possible enhanced ecosystem
282 productivity in coastal areas [37]. The Arctic region also receives additional Hg inputs from
283 melting Greenland glaciers and permafrost, processes that have been amplified by rising
284 temperatures [54, 55]. The increasing marine-Hg flux trends in the Arctic and Europe suggest
285 delayed or limited responses of the marine ecosystems to changing atmospheric Hg
286 deposition. We also acknowledge that the above analyses of marine-Hg fluxes are limited by
287 the smaller number of marine cores (25 cores) compared to peat and lake cores. Therefore,
288 future studies are encouraged to provide additional validation to bolster the findings and
289 further investigate the dynamics of Hg deposition in marine environments.

290 **Responses of ice core records to changing atmospheric deposition**

291 *Ice cores generally underrecorded atmospheric Hg deposition*

292 Similar to marine cores, Hg fluxes in ice cores also significantly differed from modelled
293 atmospheric deposition in trends and magnitudes. Comparing magnitudes to modelled total
294 atmospheric Hg deposition fluxes, 66% of ice-Hg fluxes from 1980 to 2012 showed
295 disparities exceeding ten-fold, with only 10% within a one-fold range. In general, ice-Hg
296 fluxes were nine times smaller than modelled deposition (SI Fig. S14). The GAM impact
297 factor analysis revealed that the elevation of the sampling location exerted the most
298 significant impact. This finding is likely due to higher elevations correlating with heightened
299 ultraviolet intensity, which could linearly influence the photoreduction process of Hg in ice
300 deposits [56], leading to the loss of deposited Hg. Eventually, all the differences in trends and
301 magnitudes, along with the primary impact factor, suggest that ice-Hg fluxes are unlikely to
302 respond promptly or consistently to changes in atmospheric deposition.

303 *High-altitude ice records were prone to natural influences*

304 In the ice-covered mountainous regions of Central Asia, ice-Hg fluxes remained constantly
305 low until the 1930s and then increased rapidly until 1960. Following this period, the fluxes
306 fluctuated around 0.001 mg/m²/year until 2012. The post-1960 trend of ice-Hg fluxes

307 diverged from the rising trends of both global and regional Hg emissions that affect Central
308 Asia [45]. The fluctuations in ice-Hg fluxes may result from several factors, including the loss
309 of deposited Hg through photoreduction, which is intensified by high ultraviolet radiation at
310 elevated altitudes. Additionally, these fluctuations might result from the release of stored
311 historical Hg as ice melting, driven by rising temperatures, which are particularly pronounced
312 in high-altitude regions [57, 58]. Nevertheless, the current analysis is limited by the small
313 number of ice cores available in this region (just 2 cores). More ice cores are needed to
314 improve the robustness of the trend analysis and provide more convincing evidence.

315 **Reflections of natural archive responses on global mercury management**

316 *Revisit the anthropogenic emissions during the 18th-19th centuries*

317 Several global estimates on Hg emissions in the 18th and 19th centuries revealed an unimodal
318 curve with a peak matching contemporary levels [2, 59], largely driven by silver [60],
319 mercury, and gold mining [2] during the Spanish colonization (1570-1850) and Gold Rush era
320 (1800 onwards). These high historical estimates were considered overestimated and strongly
321 contested by geochemical records [53, 61, 62]. Our synthesised regional lake-Hg fluxes in
322 Central Asia and Latin America (**Fig. 2h**) during the period showed mildly elevated lake-Hg
323 fluxes, supporting the notion that mining emissions were likely overestimated and/or had only
324 local impacts. Consequently, some studies revised these emissions to 1/3 to 1/2 of the original
325 estimates [53, 63], using natural archive Hg accumulation fluxes as references. However, it is
326 important to note the influence of sampling locations. If the distances between natural
327 archives and mining locations exceed the local impact range (typically 50 km [64] to 100 km
328 [22]), the natural archive Hg fluxes might be biased when evaluating and calibrating the
329 mining Hg emissions. Notably, no cores from California, United States — the hotbed of the
330 Gold Rush — were analysed by Zhang et al. [53] or Engstrom et al. [62], nor were any
331 included in this study. An accurate estimate of historical mining Hg emissions is crucial for
332 contemporary Hg management, as legacy Hg pollution can still influence current Hg
333 biogeochemical cycling [63]. Hence, for the further revision of the mining emissions, the use
334 of natural archive fluxes for validation or calibration should be approached with caution and
335 additional core samples are needed in key mining areas.

336 *Effectiveness of pollution control policies and impact of coal use*

337 The lake-Hg and peat-Hg fluxes in three regional groups 1) Europe, 2) North America, and 3)
338 East Asia, Africa, and Oceania provide a clear basis for comparing the effectiveness of
339 environmental policies. Both Europe and North America pioneered environmental
340 management but exhibited different pollution trajectories. In Europe, contemporary lake-Hg

341 and peat-Hg fluxes had almost returned to pre-industrial levels, indicating effective ecosystem
342 recovery and the success of pollution control measures. In contrast, the declining trends of
343 lake-Hg and peat-Hg fluxes in North America were insignificant. This discrepancy is likely
344 due to the reliance on coal, a major Hg emission source. European countries decoupled their
345 economies from coal use early on, whereas the United States maintained its reliance until
346 2008 (SI Fig. S16). A more profound impact of coal use is evident in East Asia, Africa, and
347 Oceania, where coal remained a primary energy source at least until 2012. Consequently,
348 lake-Hg fluxes in these regions showed monotonic increases, with East Asia emerging as a
349 particularly intensified Hg accumulation hotspot. The comparison results underscore that
350 general environmental policies can be effective in managing Hg pollution; however, the
351 ongoing use of coal significantly undermines this effectiveness.

352 *Critical ecosystems for Hg pollution recovery*

353 Compared to terrestrial lake and peat ecosystems, marine ecosystems are more challenging to
354 recover from Hg contamination. This is evidenced by the substantially reduced contemporary
355 Hg fluxes in lake and peat cores in Europe, whereas marine core fluxes in the same region
356 continued to rise. The difficulties in change partly stem from the fact that marine ecosystems,
357 including ocean water bodies and sediments, represent the largest Hg sink on Earth [1].
358 Additionally, the open nature of marine systems, with ocean currents mobilising Hg both
359 horizontally and vertically, significantly diminishes the effectiveness of environmental
360 policies focusing on reducing atmospheric Hg emissions and deposition on marine ecosystem
361 recovery.

362 High-altitude ecosystems face similar challenges. They are more susceptible to environmental
363 and geographical factors, making recovery difficult through the sole control of anthropogenic
364 Hg emissions. The GAM analysis indicated that elevation is the primary driving factor for
365 changing Hg fluxes in ice cores, and a secondary and tertiary factor in peat and lake cores,
366 respectively (Table 1). At higher elevations, the Hg in natural archives would be affected by
367 more presence of oxidants [47], greater photochemical reduction [56], and more intense
368 temperature increases [57, 58]. Additionally, the dynamic interactions between melting ice
369 and proglacial lakes [29, 38, 39] under climate change pose new challenges for containing Hg
370 contamination in high-altitude ecosystems.

371 **CONCLUSION**

372 In summary, we compiled a natural archive Hg record database spanning the years from 1700
373 to 2012, utilizing data from 221 cores collected from ice, peat, lake, and marine deposits
374 across eight key regions. Our analysis focused on how these natural deposits, acting as Hg

375 sinks of respective ecosystems, respond to changes in total atmospheric Hg deposition. Our
376 findings revealed that lake-Hg and peat-Hg fluxes exhibited a strong association with local
377 anthropogenic Hg emissions and mirrored the trend of total atmospheric Hg deposition, albeit
378 with higher magnitudes. This distinct characteristic evidenced the positive effect of past
379 collective environmental policies in Europe in recovering lake and peat ecosystems, at least
380 their sedimentary components, from Hg contamination. Additionally, our study revealed
381 elevated Hg accumulation in lake ecosystems in East Asia, Africa, and Oceania, likely driven
382 by economic development, including coal consumption among other factors. Conversely, ice-
383 Hg and marine-Hg fluxes were primarily regulated by natural processes, such as Hg
384 photoreductions, ice melting, and coastal erosions, and thus were not sensitive to changing
385 atmospheric inputs driven by anthropogenic interventions such as emission controls. As a
386 result, we found universal rising trends in marine-Hg fluxes in Europe and the Arctic post the
387 1950s despite declining atmospheric emissions, concentrations, and depositions. Additionally,
388 our findings underscored the challenges in containing Hg contamination in high-altitude
389 ecosystems, due to the dynamic Hg exchange and the remobilization of historical Hg through
390 ice melting.

391 Although natural deposits may not fully represent entire ecosystems, they provide valuable
392 insights into the principal responses from Hg sinks within these ecosystems, which can also
393 act as potential Hg sources. Therefore, we call for targeted mitigation strategies tailored to
394 key ecosystems in oceans and high-altitude areas, as well as critical regions such as East Asia
395 and the Arctic. Besides, it is crucial to address Hg pollution and climate change
396 simultaneously [65], as changing natural conditions—such as variations in vegetation types,
397 organism productivity, and soil erosion levels—can influence Hg contamination levels and
398 offset the effectiveness of policies. Moreover, there is a need for more paleoenvironmental
399 studies in less-explored natural archive materials, such as ice and marine sediments, and in
400 under-researched but important regions, particularly East Asia, Africa, and historical mining
401 regions. These studies are essential for enhancing our understanding of global biogeochemical
402 Hg cycling and supporting assessments of the effectiveness of Hg mitigation policies,
403 especially under the Minamata Convention on Mercury.

404 To push forward research in this direction, the established natural archive Hg database could
405 potentially help to 1) reconstruct long-time-scale, global-gridded, atmospheric Hg depositions,
406 which could be achieved by combining and complementing natural archive Hg records (long
407 temporal scale but limited in special coverage) and global modelled gridded depositions
408 (global coverage but limited in temporal scales). Successful reconstruction can provide
409 valuable Hg data for less studied areas such as East Asia, Africa and South Asia; 2)
410 incorporate with global Hg cycle modelling to constrain Hg emission estimates, including

411 anthropogenic emissions from sources like metal mining, and aquatic reemissions; 3)
412 disentangle climate and socio-economic drivers of Hg accumulation fluxes in the identified
413 key ecosystems, i.e., marine and high altitude lake systems and generate more targeted
414 policies and measures for effective ecosystem recovery from Hg contamination.

415

416 **METHODS**

417 We conducted this study following the below processes, for the detailed method, please see SI
418 Supporting Text 2 and SI Fig. S17:

- 419 1) Compiled a natural archive Hg flux database using data from lake, peat, marine, and
420 ice deposits.
- 421 2) Analysed the responses of natural archive Hg fluxes to atmospheric Hg depositions.
422 This step is divided into three parts: First, comparing natural archive Hg fluxes with
423 atmospheric Hg depositions modelled by GEOS-Chem at each coring location to
424 identify disparities and similarities. Second, examining eight key impact factors that
425 influence changes in natural archive Hg fluxes. Third, conducting spatial-temporal
426 analysis to understand the responses of natural archives in eight key regions.
- 427 3) Assessed impacts of anthropogenic activities, including environmental policies, and
428 identified critical regions and ecosystems for prioritizing future Hg abatement
429 policies.

430 This study employed a multidisciplinary approach, incorporating elements from physical
431 geography and atmospheric sciences, which resulted in uncertainties spanning various
432 dimensions. These uncertainties encompass but are not limited to the following aspects. For
433 in-depth discussions, please refer to SI Supporting Text 4.

- 434 1) Potential bias stemming from core distribution and numbers could be more
435 pronounced in regions like Southeast Asia, the Arctic, East Asia, central and southern
436 Africa, and South America. Such bias may affect the accuracy of trend and magnitude
437 analyses.
- 438 2) Uncertainties in natural archive Hg records arising from different deposition
439 mechanisms. See SI Table S1 for a summary detailing pre- and post-depositional
440 processes that contribute to differences between natural archive Hg fluxes and
441 atmospheric Hg deposition fluxes.
- 442 3) Uncertainties in natural archive Hg records arising from chronologies, including
443 dating error ranges and differences in dating methods employed across studies.

- 444 Consequently, the geochemical Hg records discussed herein should be understood as
445 representing an approximate period of ± 10 years, rather than precise years.
- 446 4) Uncertainties in natural archive Hg records arising from the concentration-to-flux
447 conversion. Contemporary Hg accumulation fluxes in ice and marine cores might be
448 underestimated due to the consistent sedimentation rates used in the conversion.
- 449 5) Uncertainties in total atmospheric Hg deposition linked to the transport and
450 deposition processes modelled in GEOS-Chem. The model employed a coarse
451 resolution of $2^{\circ} \times 2.5^{\circ}$, meaning that grid-average results might not fully represent Hg
452 deposition at specific core sampling locations. Additionally, the model might
453 underestimate total deposition onto ice surfaces and overestimate deposition onto
454 lakes due to uncertainties in high-altitude modelling and lake Hg re-emissions,
455 respectively. These uncertainties can affect the accuracy of magnitude comparisons
456 between modelled and natural archive Hg fluxes.
- 457 6) Uncertainties in Hg emission estimates on ASGM, which may further lead to
458 overestimated GEOS-Chem-modelled atmospheric deposition in East Asia, central
459 and southern Africa, and Latin America in 1980-2012.

ORIGINAL UNEDITED MANUSCRIPT

460 **RESOURCE AVAILABILITY**

461 **Materials availability**

462 The natural archive Hg flux data and core information, including references, of the selected
463 221 cores are available in Dataset S1. Ground observation data of wet mercury deposition and
464 concentrations are available in Dataset S2.

465 **Data and code availability**

466 The data used to plot Fig.1-3 are provided in Dataset S3. The GAM codes are available upon
467 reasonable request to the lead contact Shuxiao Wang (shxwang@tsinghua.edu.cn).

468 **ACKNOWLEDGEMENTS**

469 We also want to give special thanks to William Shotyk, Eichler Anja, Sarah Roberts, James
470 Zheng, Joe McConnell, Stefan Engels, Yuan Hezhong, and Takahiro Hosono, who kindly dug
471 deep on their computers and provided us with precious raw data from their papers published
472 ages ago. Some further suggested useful literature and capable researchers we should look
473 into or contact, which are of great value. This paper and the database will not be as complete
474 without their kind help.

475 **Funding**

476 This work was funded by the National Natural Science Foundation of China (2222604,
477 42394094, and 42407138), the International Postdoctoral Exchange Fellowship Program
478 (Talent Introduction Program) (YJ20210103), the Shuimu Scholar Fellowship from Tsinghua
479 University (2020SM075), and the Special fund of State Key Joint Laboratory of Environment
480 Simulation and Pollution Control (22L02ESPC).

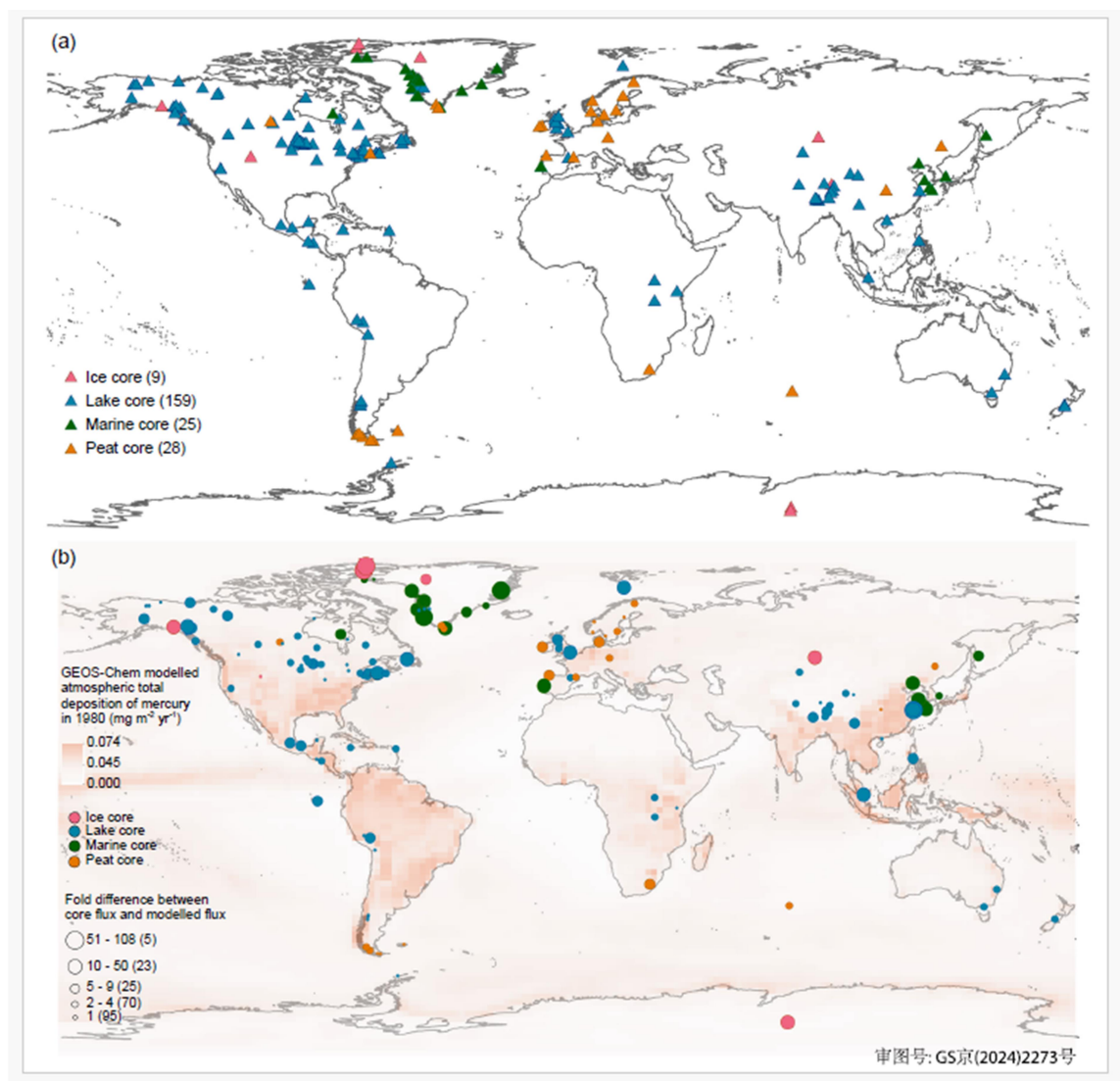
481 **AUTHOR CONTRIBUTIONS**

482 QC, QW and SW conceived the idea. QC compiled the natural archive Hg accumulation
483 database, conducted the statistical analysis, performed GAM modelling, and prepared drafts
484 and all rounds of revisions of the manuscript. QW and SW provided expertise in interpreting
485 results from Hg GEOS-Chem modelling and GAM modelling, arranged the framework of the
486 article, and provided important critiques. YC performed the GEOS-Chem Hg deposition
487 modelling and participated in the interpretation of the results. SW supervised the project and
488 was in charge of the overall study. All authors contributed to the discussion, revision and
489 edition of the manuscript.

490 **DECLARATION OF INTERESTS**

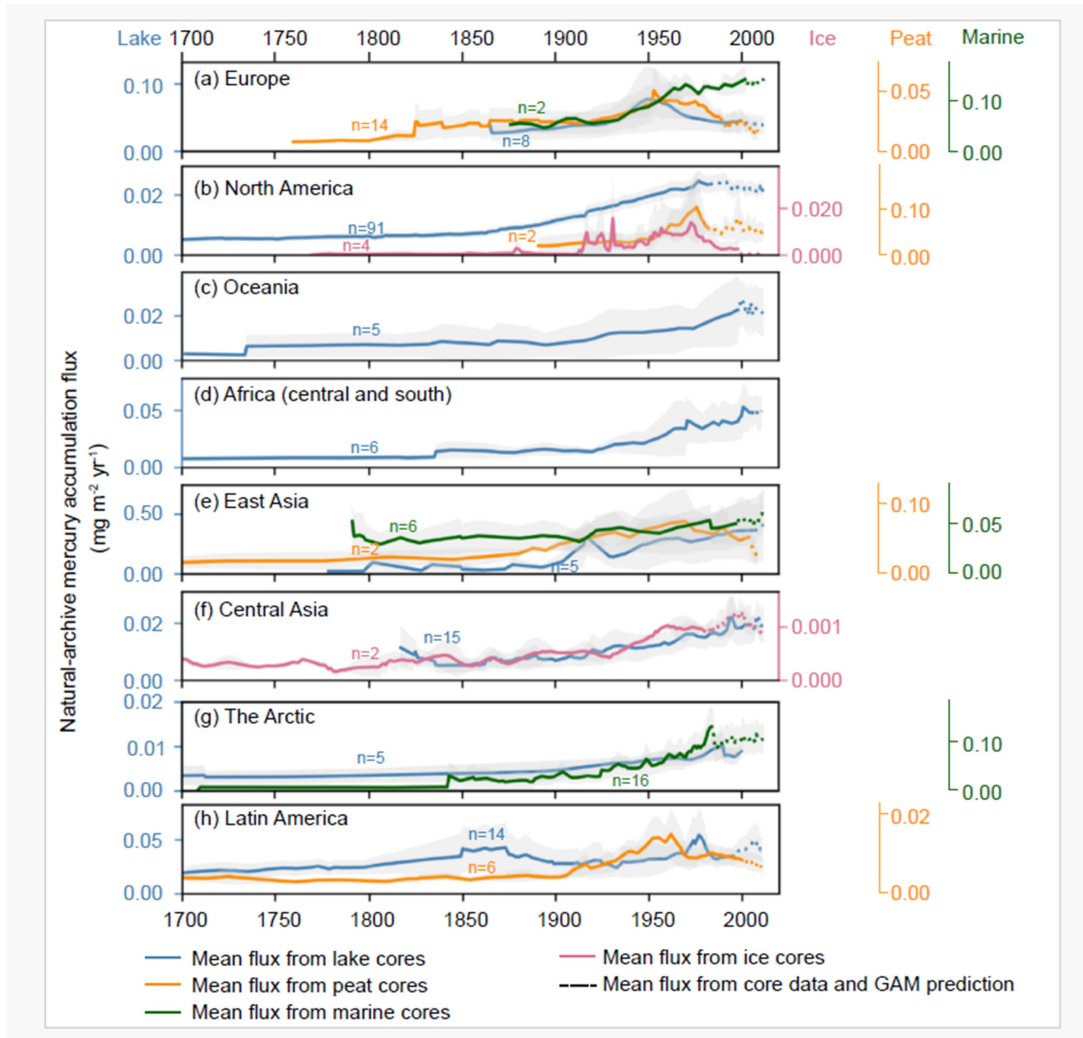
491 The authors declare no competing interests.

ORIGINAL UNEDITED MANUSCRIPT



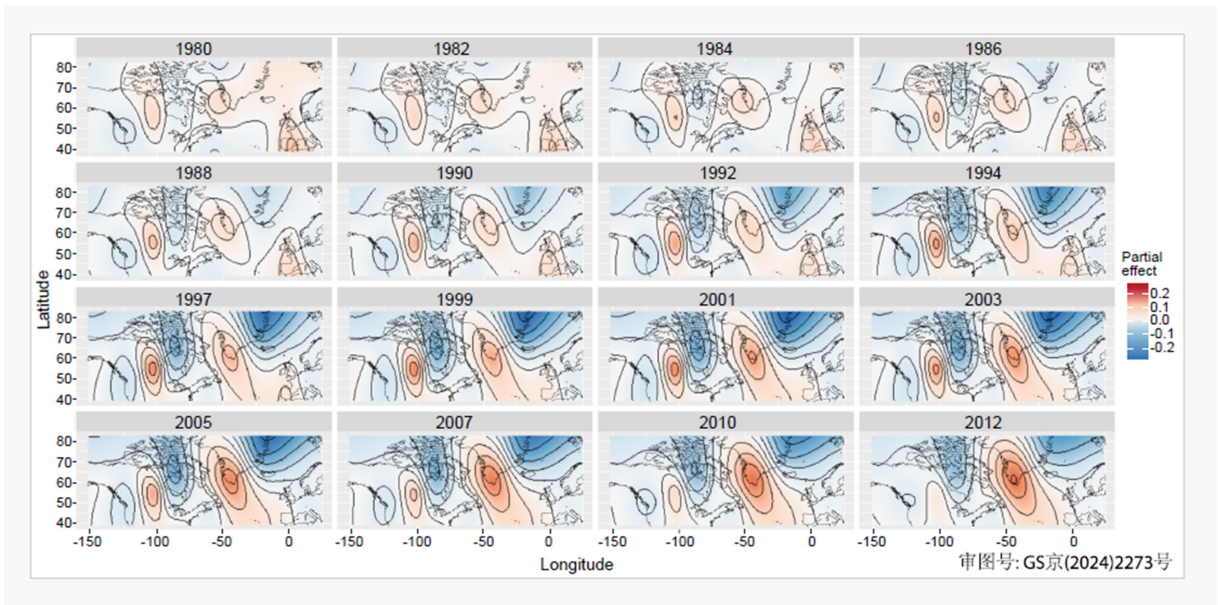
493

494 **Fig. 1** (a) Spatial distributions of natural archive records of Hg. The numbers in brackets represent
 495 the number of cores from the respective natural archives compiled in the database. Note that some
 496 cores collected from the same or nearby locations are not fully visible in the figure; please refer to
 497 Dataset S1 for detailed core information. (b) A comparison between natural archive Hg fluxes and
 498 total (wet + dry) atmospheric Hg deposition fluxes modelled by GEOS-Chem at each coring site
 499 in the base year 1980, a year with the greatest number of cores. Larger circles indicate greater
 500 disparities in magnitude. Generally, lake-Hg, peat-Hg, and marine-Hg fluxes are greater than the
 501 modelled total atmospheric Hg deposition fluxes, while ice-Hg fluxes are smaller. A total of 42%
 502 of the cores show good agreement with the modelled values, indicated by a difference within 1-
 503 fold. However, 12% of the cores exhibit differences larger than 10-fold, mostly marine and ice
 504 cores.
 505



507

508 **Fig. 2** The synthesised regional Hg accumulation fluxes reconstructed from ice, peat, lake
 509 sediments, and marine sediments from 1700 to 2012. In this context, Africa refers to central and
 510 southern areas, Oceania covers Australia and New Zealand, Latin America covers Mexico and the
 511 western Andes area, and the Arctic represents Greenland and nearby islands. The shaded areas
 512 represent 95% confidence intervals, and 'n' next to each line indicates the maximum number of
 513 cores used in plotting. Here only plotted the fluxes that were averaged from two or more cores.
 514 Dotted extended lines indicate that the fluxes were calculated using both core data and predicted
 515 values generated by the General Additive Model (GAM). The use of core + GAM predicted data
 516 aims to avoid errors induced by inconsistent numbers of cores each year, particularly after 2000,
 517 when the number of cores decreased significantly.
 518



520

521 **Fig. 3** Spatial-temporal variations in natural archive data of Hg accumulation fluxes denoted
 522 as partial effects, across North America (104 cores with 93% being lake cores), the Arctic (24
 523 cores with 67% being marine cores), and Europe (24 cores with 58% being peat cores and 33%
 524 lake cores) from 1980 to 2012, analyzed using GAM. The plots were overlaid with map
 525 contours spanning the coordinates 38N-82N, 150W-23E. The change of partial effects
 526 visually demonstrates how Hg accumulation fluxes at specific locations change along with
 527 time while holding other variables constant. This spatial-temporal GAM analysis does not
 528 distinguish between core types, aiming for a comprehensive comparison among ecosystems
 529 and geographical locations. Note that lake and peat cores are more likely to mirror total
 530 atmospheric deposition compared to marine cores. Plots show decreasing accumulation fluxes
 531 in Europe (terrestrial environment), increasing fluxes in the Arctic region (marine
 532 environment), and mixed effects in North America (terrestrial environment).

533

534

535 **Table 1** Database summary and impacts of individual changing factors on the respective natural archive Hg fluxes using general additive modelling (GAM).
 536 Star signs represent significant levels of the impacts of variables on the respective natural archive Hg records; three stars represent a level of 0.001, two stars
 537 represent a level of 0.01, and one star represents a level of 0.05. A minus sign indicates that the variable does not apply to the respective core type. Numbers
 538 in parentheses are F values. A higher F value indicates a higher effect of the variable on the respective natural archive Hg records. For graphic display see SI
 539 Figs. S7-14.

Core type	Number of cores in the database	Geographic factors		Environmental factors			Emission-related factors			Deviance explained
		Elevation/Ocean depth	Catchment area vs. lake area	Temperature	Precipitation	Greenness fraction	Local anthropogenic emission	Local non-anthropogenic emission	Global total emission	
Lake core	159	*** (36.10)	*** (62.32)	*** (60.74)	*** (5.53)	*** (37.09)	*** (76.10)	*** (37.13)	(0.00)	65.0%
Peat core	28	*** (27.32)	-	*** (16.51)	** (1.02)	*** (16.74)	*** (30.32)	*** (8.13)	*** (5.38)	88.1%
Marine core	25	*** (120.48)	-	*** (15.27)	(0.00)	-	*** (46.63)	(0.70)	(0.00)	85.2%
Ice core	9	*** (6.26)	-	*** (2.98)	(0.00)	-	-	*** (1.82)	** (1.08)	83.0%
Total	221									

ORIGINAL UNEDITED MANUSCRIPT

540 **Table 2** Spatial comparison between natural archive data of Hg accumulation fluxes and modelled total atmospheric Hg deposition fluxes (in brackets) by trend,
 541 changing rate, and magnitude. Modelled results were extracted from respective coring locations and were presented in brackets for easy comparison. ↑ indicates a
 542 general increasing trend, ↓ indicates a general decreasing trend. * indicates the trend is at a significance level of 0.05.

Core type	North America	Europe	Latin America	Oceania	Central and Southern Africa	Central Asia	East Asia	The Arctic
Trend from 1980 to 2012								
Lake core	↓ (↑*)	↓*(↓*)	↑*(↑*)	↑*(↑*)	↑*(↑*)	↑*(↑*)	↑*(↑*)	↑*(↑)
Peat core	↓ (↑*)	↓*(↓*)	↓*(↑)				↓*(↑*)	
Ice core	↓ (↑*)					↑(↑*)		
Marine core		↑(↑)					↑(↑*)	↑*(↓)
Changing rate (%/year) from 1980 to 2012								
Lake core	-0.3 (0.3)	-1.7 (-1.6)	0.4 (0.6)	1.1 (0.6)	2.2(0.8)	1.3 (0.7)	1.9 (3.7)	2.2 (0.2)
Peat core	-0.2 (0.4)	-0.4 (-0.6)	-0.6 (0.3)				-0.9 (1.8)	
Ice core	-3.5 (0.5)					0.1 (0.7)		
Marine core		0.4 (0.8)					0.6 (1.9)	0.4 (-0.2)
Mean flux (mg/m²/year) in 2012								
Lake core	0.023 (0.014)	0.039 (0.017)	0.034 (0.024)	0.021 (0.018)	0.045 (0.021)	0.020 (0.010)	0.414 (0.017)	0.007 (0.007)
Peat core	0.054 (0.011)	0.022 (0.014)	0.010 (0.017)				0.025 (0.019)	
Ice core	0.0001 (0.006)					0.001 (0.007)		
Marine core		0.144 (0.005)					0.067 (0.006)	0.108 (0.008)
Maximum number of cores								
Lake core	91	8	14	5	6	15	5	5
Peat core	2	14	6				2	
Ice core	4					2		
Marine core		2					6	16

- 544 1. UNEP. *Global Mercury Assessment 2018*. Geneva, Switzerland: United Nations
545 Environment Programme; 2019.
- 546 2. Streets DG, Horowitz HM, Jacob DJ *et al*. Total Mercury Released to the
547 Environment by Human Activities. *Environ Sci Technol*. 2017; **51**(11): 5969-5977. doi:
548 10.1021/acs.est.7b00451
- 549 3. Streets DG, Lu Z, Levin L *et al*. Historical releases of mercury to air, land, and water
550 from coal combustion. *Sci Total Environ*. 2018; **615**: 131-140. doi:
551 10.1016/j.scitotenv.2017.09.207
- 552 4. Wu Q, Zhang Y, Li P *et al*. Ecosystem Mercury Recovery and Health Benefit Under
553 the Minamata Convention in a Changing Climate. *Reviews of Environmental Contamination
554 and Toxicology*. 2022; **260**(1): 15. doi: 10.1007/s44169-022-00016-8
- 555 5. Zhang YX, Song ZC, Huang SJ *et al*. Global health effects of future atmospheric
556 mercury emissions. *Nature Communications*. 2021; **12**(1): 3035. doi: 10.1038/s41467-021-
557 23391-7
- 558 6. UNEP. Minamata Convention on Mercury, Text and Annexes. Nairobi, Kenya:
559 United Nations Environment Programme; 2019.
- 560 7. MacSween K, Stuppel G, Aas W *et al*. Updated trends for atmospheric mercury in the
561 Arctic: 1995–2018. *Sci Total Environ*. 2022; **837**: 155802. doi:
562 10.1016/j.scitotenv.2022.155802
- 563 8. Giang A, Selin NE. Benefits of mercury controls for the United States. *Proceedings
564 of the National Academy of Sciences*. 2016; **113**(2): 286-291.
- 565 9. Selin H, Selin NE. From Stockholm to Minamata and beyond: Governing mercury
566 pollution for a more sustainable future. *One Earth*. 2022; **5**(10): 1109-1125. doi:
567 10.1016/j.oneear.2022.09.001
- 568 10. Zhang Y, Jacob DJ, Horowitz HM *et al*. Observed decrease in atmospheric mercury
569 explained by global decline in anthropogenic emissions. *Proceedings of the National
570 Academy of Sciences*. 2016; **113**(3): 526-531. doi: 10.1073/pnas.1516312113
- 571 11. Jensen A, Jensen A. Historical deposition rates of mercury in scandinavia estimated
572 by dating and measurement of mercury in cores of peat bogs. *Water Air & Soil Pollution*.
573 1991; **56**(1): 769-777. doi: 10.1007/BF00342315
- 574 12. Benoit JM, Fitzgerald WF, Damman AWH. The biogeochemistry of an ombrotrophic
575 bog: Evaluation of use as an archive of atmospheric mercury deposition. *Environ Res*. 1998;
576 **78**(2): 118-133. doi: 10.1006/enrs.1998.3850
- 577 13. Percival JB, Outridge PM. A test of the stability of Cd, Cu, Hg, Pb and Zn profiles
578 over two decades in lake sediments near the Flin Flon Smelter, Manitoba, Canada. *Sci Total
579 Environ*. 2013; **454**: 307-318. doi: 10.1016/j.scitotenv.2013.03.011
- 580 14. Blais JM, Rosen MR, Smol JP. *Environmental contaminants: Using natural archives
581 to track sources and long-term trends of pollution*: Springer, 2015.
- 582 15. Hansson SV, Bindler R, De Vleeschouwer F. Using Peat Records as Natural Archives
583 of Past Atmospheric Metal Deposition. *Environmental Contaminants: Using Natural
584 Archives to Track Sources and Long-Term Trends of Pollution*. 2015; **18**: 323-354. doi:
585 10.1007/978-94-017-9541-8_12
- 586 16. Norton SA, Jacobson GL, Kopacek J *et al*. A comparative study of long-term Hg and
587 Pb sediment archives. *Environmental Chemistry*. 2016; **13**(3): 517-527. doi:
588 10.1071/En15114
- 589 17. Rausch N, Nieminen TM, Ukonmaanaho L *et al*. Retention of atmospheric Cu, Ni,
590 Cd and Zn in an ombrotrophic peat profile near the Outokumpu Cu-Ni mine, SE-Finland.
591 *JOURNAL DE PHYSIQUE IV*. 2003; **107**: 1127-1130. doi: 10.1051/jp4:20030499
- 592 18. Zhou J, Obrist D, Dastoor A *et al*. Vegetation uptake of mercury and impacts on
593 global cycling. *Nature Reviews Earth & Environment*. 2021; **2**(4): 269-284. doi:
594 10.1038/s43017-021-00146-y

- 595 19. Jiskra M, Sonke JE, Obrist D *et al.* A vegetation control on seasonal variations in
596 global atmospheric mercury concentrations. *Nature Geoscience*. 2018; **11**(4): 244-250. doi:
597 10.1038/s41561-018-0078-8
- 598 20. Verbeke BA, Lamit LJ, Lilleskov EA *et al.* Latitude, elevation, and mean annual
599 temperature predict peat organic matter chemistry at a global scale. *Global Biogeochemical*
600 *Cycles*. 2022; **36**(2): e2021GB007057. doi: 10.1029/2021GB007057
- 601 21. Shotbolt LA, Thomas AD, Hutchinson SM. The use of reservoir sediments as
602 environmental archives of catchment inputs and atmospheric pollution. *Progress in Physical*
603 *Geography*. 2005; **29**(3): 337-361.
- 604 22. Roberts SL, Kirk JL, Muir DCG *et al.* Quantification of Spatial and Temporal Trends
605 in Atmospheric Mercury Deposition across Canada over the Past 30 Years. *Environ Sci*
606 *Technol*. 2021; **55**(23): 15766-15775. doi: 10.1021/acs.est.1c04034
- 607 23. Wiklund JA, Kirk JL, Muir DCG *et al.* Anthropogenic mercury deposition in Flin
608 Flon Manitoba and the Experimental Lakes Area Ontario (Canada): A multi-lake sediment
609 core reconstruction. *Sci Total Environ*. 2017; **586**: 685-695. doi:
610 10.1016/j.scitotenv.2017.02.046
- 611 24. Lamborg CH, Hammerschmidt CR, Bowman KL *et al.* A global ocean inventory of
612 anthropogenic mercury based on water column measurements. *Nature*. 2014; **512**(7512): 65-
613 68. doi: 10.1038/nature13563
- 614 25. DiMento BP, Mason RP, Brooks S *et al.* The impact of sea ice on the air-sea
615 exchange of mercury in the Arctic Ocean. *Deep Sea Research Part I: Oceanographic*
616 *Research Papers*. 2019; **144**: 28-38. doi: 10.1016/j.dsr.2018.12.001
- 617 26. Meng M, Sun R-y, Liu H-w *et al.* An Integrated Model for Input and Migration of
618 Mercury in Chinese Coastal Sediments. *Environ Sci Technol*. 2019; **53**(5): 2460-2471. doi:
619 10.1021/acs.est.8b06329
- 620 27. Kang S, Wang F, Morgenstern U *et al.* Dramatic loss of glacier accumulation area on
621 the Tibetan Plateau revealed by ice core tritium and mercury records. *The Cryosphere*. 2015;
622 **9**(3): 1213-1222. doi: 10.5194/tc-9-1213-2015
- 623 28. Kang S, Huang J, Wang F *et al.* Atmospheric Mercury Depositional Chronology
624 Reconstructed from Lake Sediments and Ice Core in the Himalayas and Tibetan Plateau.
625 *Environ Sci Technol*. 2016; **50**(6): 2859-2869. doi: 10.1021/acs.est.5b04172
- 626 29. Zhu T, Wang X, Lin H *et al.* Accumulation of Pollutants in Proglacial Lake
627 Sediments: Impacts of Glacial Meltwater and Anthropogenic Activities. *Environ Sci Technol*.
628 2020; **54**(13): 7901-7910. doi: 10.1021/acs.est.0c01849
- 629 30. Li C, Sonke JE, Le Roux G *et al.* Unequal Anthropogenic Enrichment of Mercury in
630 Earth's Northern and Southern Hemispheres. *ACS Earth and Space Chemistry*. 2020; **4**(11):
631 2073-2081. doi: 10.1021/acsearthspacechem.0c00220
- 632 31. Goodsite ME, Outridge PM, Christensen JH *et al.* How well do environmental
633 archives of atmospheric mercury deposition in the Arctic reproduce rates and trends depicted
634 by atmospheric models and measurements? *Sci Total Environ*. 2013; **452-453**: 196-207. doi:
635 10.1016/j.scitotenv.2013.02.052
- 636 32. Cooke CA, Martínez-Cortizas A, Bindler R *et al.* Environmental archives of
637 atmospheric Hg deposition – A review. *Sci Total Environ*. 2020; **709**: 134800. doi:
638 10.1016/j.scitotenv.2019.134800
- 639 33. Lee JH, Kwon SY, Yin R *et al.* Spatiotemporal Characterization of Mercury Isotope
640 Baselines and Anthropogenic Influences in Lake Sediment Cores. *Global Biogeochemical*
641 *Cycles*. 2021; **35**(10): e2020GB006904. doi: 10.1029/2020GB006904
- 642 34. Pedersen EJ, Miller DL, Simpson GL *et al.* Hierarchical generalized additive models
643 in ecology: an introduction with mgcv. *PeerJ*. 2019; **7**: e6876.
- 644 35. Muntean M, Janssens-Maenhout G, Song S *et al.* Evaluating EDGARv4.tox2
645 speciated mercury emissions ex-post scenarios and their impacts on modelled global and
646 regional wet deposition patterns. *Atmos Environ*. 2018; **184**: 56-68. doi:
647 10.1016/j.atmosenv.2018.04.017
- 648 36. Gelaro R, McCarty W, Suárez MJ *et al.* The modern-era retrospective analysis for
649 research and applications, version 2 (MERRA-2). *J Clim*. 2017; **30**(14): 5419-5454.

- 650 37. Zhang Y, Zhang P, Song Z *et al.* An updated global mercury budget from a coupled
651 atmosphere-land-ocean model: 40% more re-emissions buffer the effect of primary emission
652 reductions. *One Earth*. 2023; **6**(3): 316-325. doi: 10.1016/j.oneear.2023.02.004
- 653 38. Perez-Rodriguez M, Biester H, Aboal JR *et al.* Thawing of snow and ice caused
654 extraordinary high and fast mercury fluxes to lake sediments in Antarctica. *Geochim
655 Cosmochim Acta*. 2019; **248**: 109-122. doi: 10.1016/j.gca.2019.01.009
- 656 39. Sun X, Zhang Q, Zhang G *et al.* Melting Himalayas and mercury export: Results of
657 continuous observations from the Rongbuk Glacier on Mt. Everest and future insights. *Water
658 Res*. 2022; **218**: 118474. doi: 10.1016/j.watres.2022.118474
- 659 40. Crippa M, Janssens-Maenhout G, Dentener F *et al.* Forty years of improvements in
660 European air quality: regional policy-industry interactions with global impacts. *Atmospheric
661 Chemistry and Physics*. 2016; **16**(6): 3825-3841.
- 662 41. Weiss-Penzias PS, Gay DA, Brigham ME *et al.* Trends in mercury wet deposition
663 and mercury air concentrations across the U.S. and Canada. *Sci Total Environ*. 2016; **568**:
664 546-556. doi: 10.1016/j.scitotenv.2016.01.061
- 665 42. bp. bp Statistical Review of World Energy - all data. 2022.
- 666 43. Verbrugge B, Geenen S. Global Gold Production Touching Ground: Expansion,
667 Informalization, and Technological Innovation. Cham: Cham: Springer International
668 Publishing; 2020.
- 669 44. Veiga MM, Fadina O. A review of the failed attempts to curb mercury use at artisanal
670 gold mines and a proposed solution. *The Extractive Industries and Society*. 2020; **7**(3): 1135-
671 1146. doi: 10.1016/j.exis.2020.06.023
- 672 45. Yu B, Yang L, Liu H *et al.* Tracing the Transboundary Transport of Mercury to the
673 Tibetan Plateau Using Atmospheric Mercury Isotopes. *Environ Sci Technol*. 2022; **56**(3):
674 1568-1577. doi: 10.1021/acs.est.1c05816
- 675 46. Weigelt A, Ebinghaus R, Pirrone N *et al.* Tropospheric mercury vertical profiles
676 between 500 and 10 000 m in central Europe. *Atmospheric Chemistry and Physics*. 2016;
677 **16**(6): 4135-4146. doi: 10.5194/acp-16-4135-2016
- 678 47. Yang H, Battarbee RW, Turner SD *et al.* Historical Reconstruction of Mercury
679 Pollution Across the Tibetan Plateau Using Lake Sediments. *Environ Sci Technol*. 2010;
680 **44**(8): 2918-2924. doi: 10.1021/es9030408
- 681 48. Zheng J. Archives of total mercury reconstructed with ice and snow from Greenland
682 and the Canadian High Arctic. *Sci Total Environ*. 2015; **509**: 133-144.
- 683 49. Huang J, Kang S, Zhang Q *et al.* Spatial distribution and magnification processes of
684 mercury in snow from high-elevation glaciers in the Tibetan Plateau. *Atmos Environ*. 2012;
685 **46**: 140-146. doi: 10.1016/j.atmosenv.2011.10.008
- 686 50. Thiagarajan N, McManus JF. Productivity and sediment focusing in the Eastern
687 Equatorial Pacific during the last 30,000 years. *Deep Sea Research Part I: Oceanographic
688 Research Papers*. 2019; **147**: 100-110. doi: 10.1016/j.dsr.2019.03.007
- 689 51. Martin J, Sanchez-Cabeza JA, Eriksson M *et al.* Recent accumulation of trace metals
690 in sediments at the DYFAMED site (Northwestern Mediterranean Sea). *Mar Pollut Bull*.
691 2009; **59**(4-7): 146-153. doi: 10.1016/j.marpolbul.2009.03.013
- 692 52. Cossa D, Knoery J, Bănaru D *et al.* Mediterranean Mercury Assessment 2022: An
693 Updated Budget, Health Consequences, and Research Perspectives. *Environ Sci Technol*.
694 2022; **56**(7): 3840-3862. doi: 10.1021/acs.est.1c03044
- 695 53. Zhang Y, Jaeglé L, Thompson L *et al.* Six centuries of changing oceanic mercury.
696 *Global Biogeochemical Cycles*. 2014; **28**(11): 1251-1261. doi: 10.1002/2014GB004939
- 697 54. Dastoor A, Angot H, Bieser J *et al.* Arctic mercury cycling. *Nature Reviews Earth &
698 Environment*. 2022; **3**(4): 270-286. doi: 10.1038/s43017-022-00269-w
- 699 55. Asmund G, Nielsen SP. Mercury in dated Greenland marine sediments. *Sci Total
700 Environ*. 2000; **245**(1): 61-72. doi: 10.1016/S0048-9697(99)00433-7
- 701 56. Mann EA, Mallory ML, Ziegler SE *et al.* Mercury in Arctic snow: Quantifying the
702 kinetics of photochemical oxidation and reduction. *Sci Total Environ*. 2015; **509**: 115-132.
703 doi: 10.1016/j.scitotenv.2014.07.056

- 704 57. Mountain Research Initiative EDW Working Group. Elevation-dependent warming in
705 mountain regions of the world. *Nature climate change*. 2015; **5**(5): 424-430.
- 706 58. Guo D, Yu E, Wang H. Will the Tibetan Plateau warming depend on elevation in the
707 future? *Journal of Geophysical Research: Atmospheres*. 2016; **121**(8): 3969-3978.
- 708 59. Streets DG, Devane MK, Lu Z *et al*. All-Time Releases of Mercury to the
709 Atmosphere from Human Activities. *Environ Sci Technol*. 2011; **45**(24): 10485-10491. doi:
710 10.1021/es202765m
- 711 60. Camargo JA. Contribution of Spanish–American silver mines (1570–1820) to the
712 present high mercury concentrations in the global environment: a review. *Chemosphere*. 2002;
713 **48**(1): 51-57.
- 714 61. AMAP/UNEP. *Technical Background Report for the Global Mercury Assessment*
715 *2018*. Arctic Monitoring and Assessment Programme, Oslo, Norway/UN Environment
716 Programme, Chemicals and Health Branch, Geneva, Switzerland; 2019.
- 717 62. Engstrom DR, Fitzgerald WF, Cooke CA *et al*. Atmospheric Hg Emissions from
718 Preindustrial Gold and Silver Extraction in the Americas: A Reevaluation from Lake-
719 Sediment Archives. *Environ Sci Technol*. 2014; **48**(12): 6533-6543. doi: 10.1021/es405558e
- 720 63. Guerrero S, Schneider L. The global roots of pre-1900 legacy mercury. *Proceedings*
721 *of the National Academy of Sciences*. 2023; **120**(31): e2304059120. doi:
722 10.1073/pnas.2304059120
- 723 64. Gerson JR, Szponar N, Zambrano AA *et al*. Amazon forests capture high levels of
724 atmospheric mercury pollution from artisanal gold mining. *Nature Communications*. 2022;
725 **13**(1): 559. doi: 10.1038/s41467-022-27997-3
- 726 65. UNEP. *Chemicals, Wastes and Climate change: Interlinkages and Potential for*
727 *Coordinated Action*. Geneva, Switzerland: United Nations Environment Programme; 2021.

728

ORIGINAL UNEDITED MANUSCRIPT